# The ubiquitin proteasome system in Huntington disease : impairment of the proteolytic machinery aggravates huntingtin aggregation and toxicity

Pril, R. de

# Chapter 3

## Accumulation of aberrant ubiquitin induces aggregate formation and cell death in polyglutamine diseases

Remko de Pril, David F. Fischer, Marion L.C. Maat-Schieman,
Barbara Hobo, Rob A.I. de Vos, Ewout R. Brunt, Elly M. Hol,
Raymund A.C. Roos and Fred W. van Leeuwen

*Hum Mol Genet* **13:** 1803-1813

## Abstract

Polyglutamine diseases are characterized by neuronal intranuclear inclusions of expanded polyglutamine proteins, indicating failing protein degradation. UBB$^{+1}$, an aberrant form of ubiquitin, is a substrate and inhibitor of the proteasome, and was previously reported to accumulate in Alzheimer disease and other tauopathies. Here we show accumulation of UBB$^{+1}$ in the neuronal intranuclear inclusions and the cytoplasm of neurons in Huntington disease and spinocerebellar ataxia type 3, indicating inhibition of the proteasome by polyglutamine proteins in human brain. We found that UBB$^{+1}$ not only increased aggregate formation of expanded polyglutamines in neuronally differentiated cell lines, but also had a synergistic effect on apoptotic cell death due to expanded polyglutamine proteins. These findings implicate UBB$^{+1}$ as an aggravating factor in polyglutamine-induced neurodegeneration, and clearly identify an important role for the ubiquitin-proteasome system in polyglutamine diseases.

## Introduction

At least nine different neurodegenerative diseases are known that are caused by the expansion of a CAG repeat in the coding region of a transcribed gene, including the spinocerebellar ataxias (SCAs) and Huntington disease (HD) (Nakamura et al., 2001; Zoghbi and Orr, 2000). All these CAG expansion diseases are characterized by progressive neuronal dysfunction starting around adult-life and resulting in severe neurodegeneration. In the channelopathy SCA6, neurodegeneration is caused by a small CAG expansion (to 19-30 repeats) in a calcium channel subunit that presumably causes a change of function (Zhuchenko et al., 1997). The other eight diseases are probably caused by a gain of function of the proteins carrying the expanded polyglutamine repeat. The pathological repeat length for these genuine polyglutamine expansion disorders starts around 40 glutamine repeats in the affected gene, with increasing severity and earlier manifestation upon greater expansion (Zoghbi and Orr, 2000).

One of the hallmarks of the pathology of polyglutamine diseases is the formation of neuronal intranuclear inclusions (NIIs) in the affected areas of the brain (DiFiglia et al., 1997). Although many of the proteins carrying the polyglutamine repeat have a cytoplasmic function, upon polyglutamine expansion they all form intranuclear inclusions that contain at least the expanded polyglutamine fragment. In HD, for instance, the NIIs contain only the N-terminal part of huntingtin with the polyglutamine stretch (DiFiglia et al., 1997; Maat-Schieman et al., 1999; Sieradzan et al., 1999; Zhou et al., 2003). The major pathological difference between the polyglutamine diseases is the regional distribution of neurodegeneration. In HD the striatum is the most severely affected area and the cortex is affected to a lesser extent (Halliday et al., 1998). In SCA3, in contrast, neuronal degeneration occurs primarily in the nuclei of the brainstem and the spinal cord (Takiyama et al., 1994). This regional specificity is probably caused by differences in expression levels of the respective disease genes among the various brain regions or different vulnerability of various types of neurons. In addition to the repeat expansion, other factors, such as proteasomal activity and expression or recruitment of cellular chaperones, probably influence polyglutamine toxicity and disease development (Chan et al., 2002; Wexler et al., 2004; Willingham et al., 2003).

NIIs contain ubiquitin or ubiquitinated proteins, which indicates that the aggregating proteins are targeted to, but not degraded by, the proteasome (DiFiglia et al., 1997; Paulson et al., 1997). In vitro studies have furthermore shown that expanded polyglutamines can directly inhibit the proteasome (Bence et al., 2001; Verhoef et al., 2002). In addition, in SCA3 patients, subunits of the 26S proteasome have been shown to be recruited to NIIs (Chai et al., 1999; Schmidt et al., 2002). Finally, in SCA1 transgenic mice, the Purkinje cell pathology was aggravated by mutation of the E6-AP ubiquitin ligase (Cummings et al., 1999). All these findings point towards an involvement of the ubiquitin-proteasome system (UPS) in the pathogenesis of

***Figure 1: UBB$^{+1}$ colocalizes with polyglutamine proteins in HD and SCA3.***

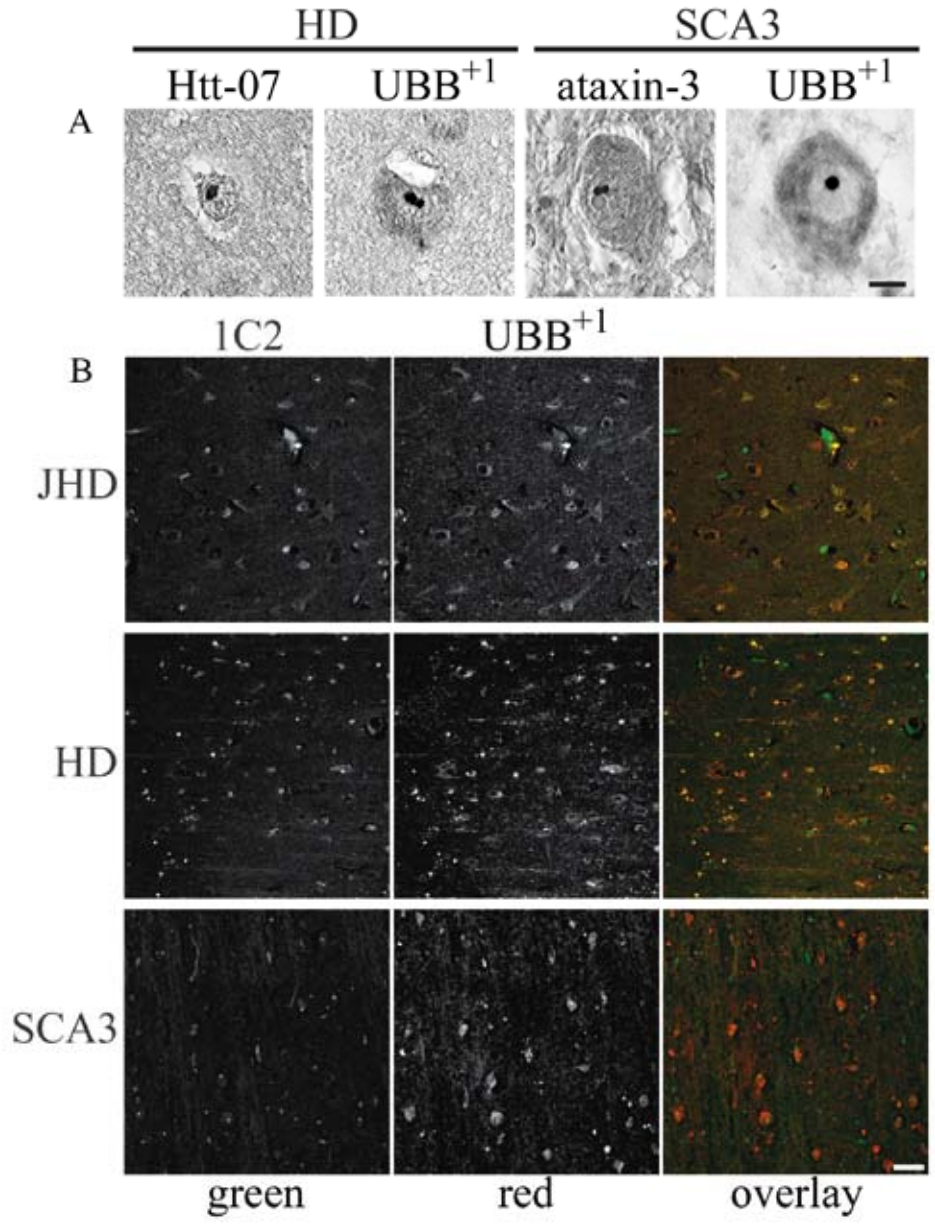


*Staining of paraffin sections of the frontal cortex of HD patients and the pons of SCA3 patients for UBB$^{+1}$ and respectively Htt-07 and α-ataxin-3 (A). Pictures show staining of NIIs with UBB$^{+1}$, distinct from the nucleoli, in both polyglutamine diseases. Magnification bar is 10μm. Double stainings show UBB$^{+1}$ staining in all inclusions positive for 1C2 in juvenile as well as late onset HD and SCA3 (B). Magnification bar is 50μm. Note also the cytoplasmic staining for UBB$^{+1}$ in both disorders (A and B).*

polyglutamine diseases and to an enhancement of neurodegeneration by further impairment of the UPS (Ciechanover and Brundin, 2003).

We previously reported that, in Alzheimer disease (AD), an aberrant form of ubiquitin (UBB$^{+1}$) accumulates in the neuropathological hallmarks of the disease (van Leeuwen et al., 1998). This UBB$^{+1}$ protein is formed by a dinucleotide deletion (ΔGU), leading to a +1 reading frame in the mRNA, and subsequent translation to a protein with an aberrant C-terminus. Thus far UBB$^{+1}$ protein has been found in the hallmarks of several neurodegenerative diseases, including AD and other tauopathies, whereas it was not detected in synucleinopathies and young control patients without pathology (Fischer et al., 2003; van Leeuwen et al., 1998). The aberrant transcript however, in contrast to the protein, appeared to be present even in young controls. Under normal circumstances, neurons can apparently cope with UBB$^{+1}$, and accumulation of this protein reflects proteasomal dysfunction in different neuropathologal disorders (Fischer et al., 2003).

*In vitro* studies have shown that, although UBB$^{+1}$ can be degraded by the proteasome (Fischer et al., 2003; Lindsten et al., 2002), at higher concentrations it inhibits proteasomal degradation of cellular proteins and leads to cell death in neuroblastoma cells (De Vrij et al., 2001; Lam et al., 2000). In addition, UBB$^{+1}$ has recently been implicated to mediate neurodegeneration via downstream interaction with the E2-25K ubiquitin conjugating enzyme, which induces amyloid-β neurotoxicity *in vitro* (Song et al., 2003). In this perspective, UBB$^{+1}$ might accelerate disease progression and increase the severity of the disease. Notably, recent reports show that the proteasome activity is indeed decreased in AD (Keck et al., 2003; Keller et al., 2000), strengthening the idea that UBB$^{+1}$ accumulation is intimately related to impairment of the proteasome (Ciechanover and Brundin, 2003).

Different findings point towards defective protein degradation in polyglutamine diseases. We examined post-mortem brain material of HD and SCA3 for the accumulation of UBB$^{+1}$, as a marker for proteasomal impairment. Moreover, we used a cellular model for polyglutamine disease to study the contribution of UBB$^{+1}$ to disease progression, i.e. polyglutamine aggregation and cell death.

## Results

To identify NIIs in different brain areas of HD and SCA3, we used antibodies against the N-terminal fragment of the huntingtin protein or full length ataxin-3 respectively (Figure 1A). In addition, we used an ubiquitin antibody and the 1C2 antibody to identify the inclusions. SCA6 showed staining of cytoplasmic aggregates with the α1A-subunit antibody (data not shown).

***Figure 2: UBB$^{+1}$ colocalizes with expanded polyglutamines in vitro.***

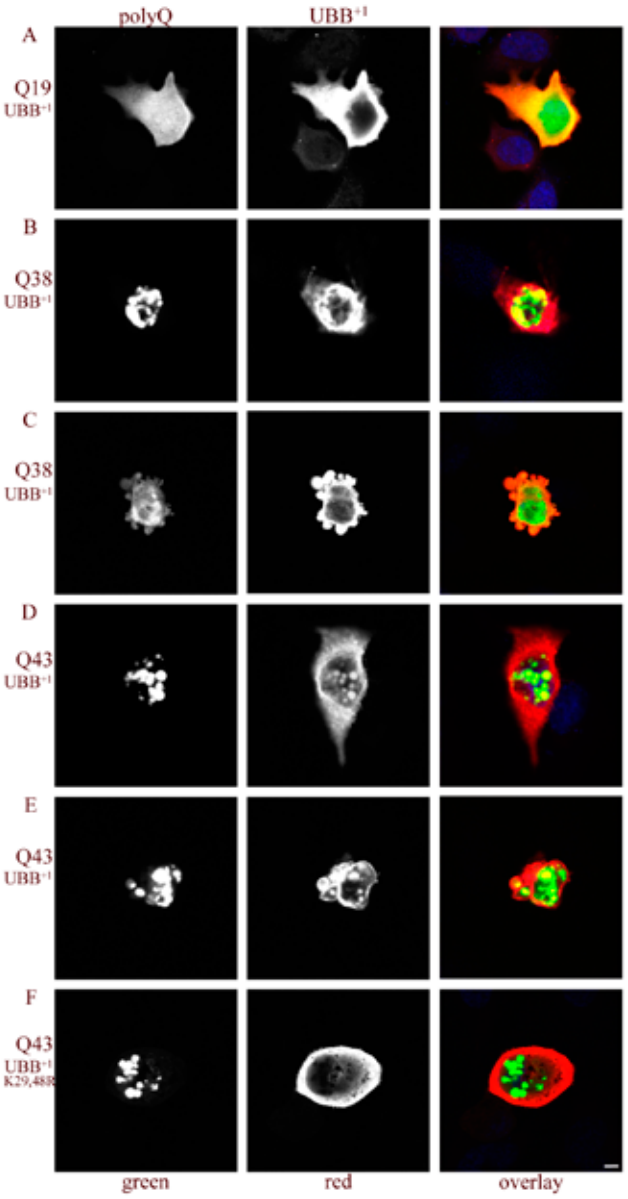


*HeLa cells co-transfected with plasmids with a truncated huntingtin fragment containing 19, 38 or 43 glutamine repeats (HA-Q-GFP) together with constructs for UBB$^{+1}$ or UBB$^{+1;K29,48R}$, were fixed 4 days post transfection. All cells that were transfected with the construct with 19 glutamines showed a diffuse cellular polyglutamine staining (A; green; left panel). Constructs with 38 and 43 glutamine repeats result in the formation of multiple polyglutamine aggregates (respectively B-C, and D-F; green; left column). Co-transfection with UBB$^{+1}$ gave cytoplasmic staining for UBB$^{+1}$ (A-E) (in red; middle column) with all constructs. In addition, UBB$^{+1}$ co-aggregates with the polyglutamine constructs Q38 (B and C) and Q43 (D and E) whereas UBB$^{+1;K29,48R}$ only shows cytoplasmic staining despite aggregate formation of Q43 (F). The right column shows the overlay of UBB$^{+1}$ and polyglutamine, with faint To-Pro nuclear staining in blue. Magnification bar is 10μm.*

With antibodies against the UBB$^{+1}$ protein, we detected immunopositive NIIs in the cortex (Figure 1A) and striatum of all HD patients (*N*=30). We found accumulation of UBB$^{+1}$ not only in adult-onset patients but already in juvenile HD. Furthermore, we detected UBB$^{+1}$ immunopositive NIIs in all SCA3 patients (*N*=6), in all the areas investigated (Figure 1A). Besides localization to the NIIs, we also found cytoplasmic staining for UBB$^{+1}$ in the affected neurons in HD and SCA3 (Figure 1A). In contrast, in the SCA6 patients (*N*=2) we did not find any UBB$^{+1}$ staining in the affected regions (data not shown). To ascertain whether UBB$^{+1}$ localizes to all or only a subset of NIIs stained with 1C2 we performed double immunofluorescent stainings on tissue sections of both HD and SCA3. We found colocalization of polyglutamine proteins and UBB$^{+1}$ in all the inclusions that were found in both HD and SCA3 (Figure 1B). Accumulation of UBB$^{+1}$ is thus not specific for HD but a general phenomenon found in polyglutamine diseases.

Besides being a marker for proteasome impairment, *in vitro*, UBB$^{+1}$ inhibits the proteasome (Lam et al., 2000; Lindsten et al., 2002). Constructs with expanded polyglutamine repeats can be used to mimic many of the features of polyglutamine diseases in cell lines, including aggregate formation and interaction with other proteins (Cummings et al., 1999; de Cristofaro et al., 1999; Hackam et al., 1999; Lunkes and Mandel, 1998).

To investigate the impact of UBB$^{+1}$ protein on aggregate formation we used plasmids with a truncated huntingtin fragment containing 19, 38 or 43 glutamine repeats (HA-Q19-GFP, HA-Q38-GFP and HA-Q43-GFP) in combination with plasmids containing either UBB$^{+1}$ or a lysine mutant of UBB$^{+1}$ (UBB$^{+1;K29,48R}$), that does not inhibit the proteasome (Lindsten et al., 2002). Co-transfection of UBB$^{+1}$ with Q19 resulted in distribution of Q19 throughout the cells and cytoplasmic staining for UBB$^{+1}$ (Figure 2A). However, besides accumulation of UBB$^{+1}$ in cells with expanded polyglutamine proteins we found colocalization with the inclusions of Q38 (Figure 2B and C) and Q43 (Figure 2D and E). The nuclear localization of the aggregates in these cells was similar to what was observed in post-mortem brain material of the different polyglutamine diseases. In addition, a number of cells display a clear apoptotic morphology, with fragmented nuclei (Figure 2C and E), in agreement with previous findings for UBB$^{+1}$ or expanded polyglutamines alone (De Vrij et al., 2001; Lunkes and Mandel, 1998). In contrast to UBB$^{+1}$, after transfection with UBB$^{+1;K29,48R}$ we found no colocalization with the aggregating polyglutamines (Figure 2F; Q43). It is remarkable that this latter ubiquitin mutant is not incorporated in the inclusions, although cytoplasmic levels are higher than for UBB$^{+1}$ transfected cells (Lindsten et al., 2002).

For functional characterizations we used neuronally-differentiated human neuroblastoma cells (SH-SY5Y) (Encinas et al., 2000). Cell-proliferation markedly influences the aggregate formation and cell-death (Yoshizawa et al., 2001), which makes differentiated cells a more useful model for functional assays. In our experiments, HeLa cells showed comparable aggregate formation, but due to proliferation and susceptibility, much lower levels of cell-death (data not shown).

We quantified the aggregate formation after lentiviral transduction of SH-SY5Y neuroblastoma cells with polyglutamine vectors in combination with $UBB^{+1}$ or the double lysine mutant of $UBB^{+1}$ (Figure 3A). The truncated huntingtin fragments with 38 or 43 glutamines show a marked increase in aggregate formation under the influence of $UBB^{+1}$ in comparison to $UBB^{+1;K29,48R}$. Accumulation of $UBB^{+1}$ causes an increase in polyglutamine protein and thus enhances the aggregate formation. For the huntingtin fragment with 38 glutamines we even find a doubling of the number of aggregate forming cells due to $UBB^{+1}$ from 4 days on (Figure 3A). Statistical analysis by three-way ANOVA confirmed a highly significant correlation between the aggregate formation, the influence of $UBB^{+1}$ and the time course ($P$<0.001). Immunofluorescent stainings furthermore show a preferential accumulation of $UBB^{+1}$ in the cells with the expanded huntingtin fragments (Figure 3B). Quantification of the cells 4 days after infection showed a clear increase in the amount of $UBB^{+1}$ expressing cells upon expansion of the polyglutamine repeat (Figure 3B). Statistical analysis by one-way ANOVA confirmed a highly significant correlation between the repeat expansion and $UBB^{+1}$ accumulation ($P$=0.001).

***Figure 3: $UBB^{+1}$ induces aggregate formation and preferentially accumulates with expanded polyglutamines.***

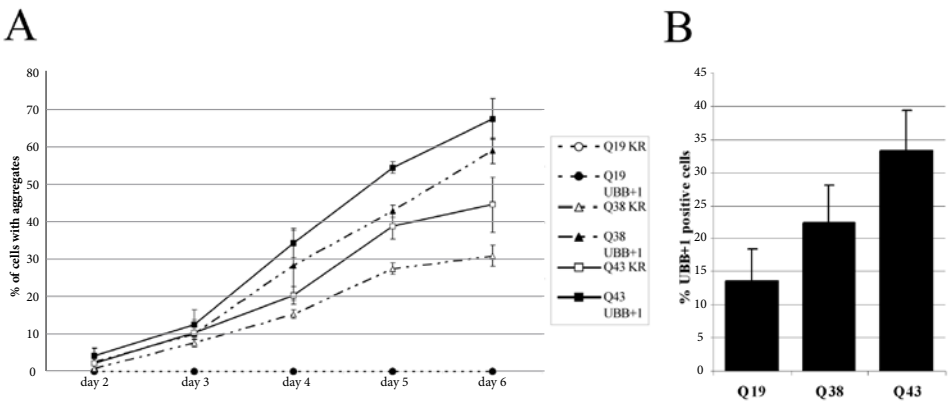


*Differentiated SH-SY5Y neuroblastoma cells were lentivirally infected with constructs with truncated huntingtin fragments containing 19, 38 or 43 glutamine repeats (HA-Q-GFP) in combination with either $UBB^{+1;K29,48R}$ (KR) or $UBB^{+1}$ (+1). Cells were quantified for aggregate formation every 24 hours after infection (A). Note that huntingtin with 19 glutamines does not result in the formation of aggregates, resulting in two overlapping lines in this graph. Constructs with 38 and 43 glutamines both show a marked increase in the number of aggregate forming cells in the presence of $UBB^{+1}$. Statistical analysis by three-way ANOVA demonstrated a strong correlation between the aggregate formation of expanded polyglutamines, the influence of $UBB^{+1}$ and the time course (P<0.001). Expression of $UBB^{+1}$ was quantified 4 days after infection (B). The expression of expanded huntingtin fragments causes a preferential accumulation of $UBB^{+1}$ in these cells. Statistical analysis by one-way ANOVA showed a highly significant correlation between repeat expansion of the huntingtin fragments and the $UBB^{+1}$ accumulation (P=0.001). All experiments were performed in triplicate.*

We made cell lysates 6 days after infection and analyzed these by Western blotting (Figure 4). Western blots probed with an anti-HA antibody showed, due to UBB$^{+1}$, a threefold increase in SDS-insoluble aggregate fraction at the top of the gel with both 38 and 43 glutamines (Figure 4A). The amounts of soluble polyglutamine protein however, show only a slight increase for all repeat lengths (Figure 4B). The bars (Figure 4D) represent the relative amount of aggregates (Figure 4A) after correction for β-actin (Figure 4C). Statistical analysis by two-way ANOVA confirmed that UBB$^{+1}$ has a pronounced, highly significant synergistic effect on the aggregate formation of constructs with 38 and 43 glutamines ($P$<0.001).

***Figure 4: UBB$^{+1}$ increases aggregate formation of expanded polyglutamines.***

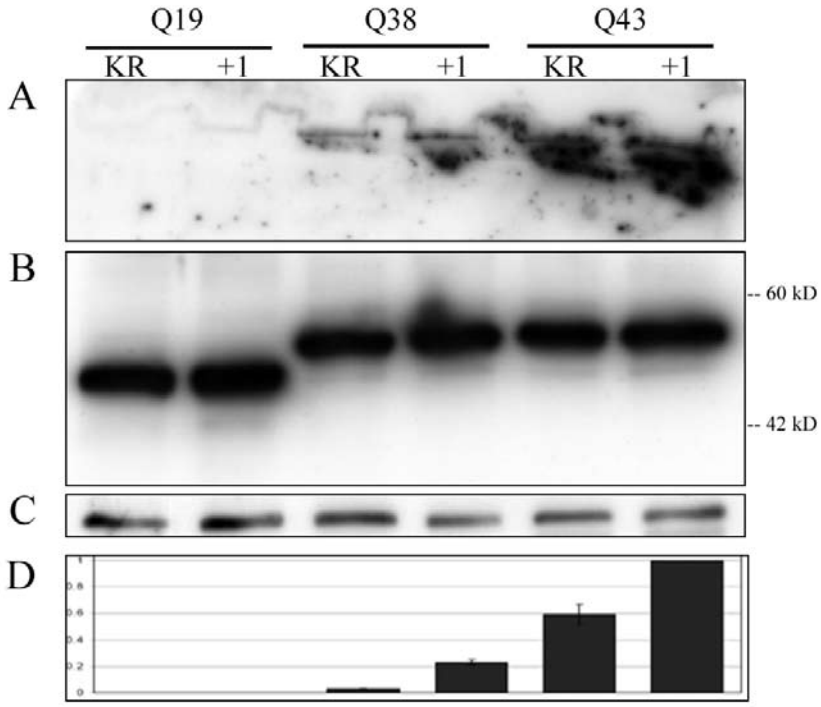


*Differentiated SH-SY5Y neuroblastoma cells were lentivirally infected with constructs with truncated huntingtin fragments containing 19, 38 or 43 glutamine repeats (HA-Q-GFP) in combination with either UBB$^{+1;K29,48R}$ (KR) or UBB$^{+1}$ (+1), and harvested 6 days after infection. Especially with 38 glutamines a marked increase is seen in the SDS-insoluble fraction that is retained at the top of the gel when cells are co-infected with UBB$^{+1}$ (A). The levels of soluble polyglutamine protein show a minor increase (B, around 60kD). Panel (C) shows a β-actin staining as a loading control. Bars show the relative integrated optical densities of the aggregate fraction after correction for loading (D). Statistical analysis by two-way ANOVA showed a strong synergistic effect of UBB$^{+1}$ on aggregate formation by expanded polyglutamines (P<0.001). All experiments were performed in triplicate.*

***Figure 5: UBB$^{+1}$ synergistically aggravates polyglutamine-induced cell death.***

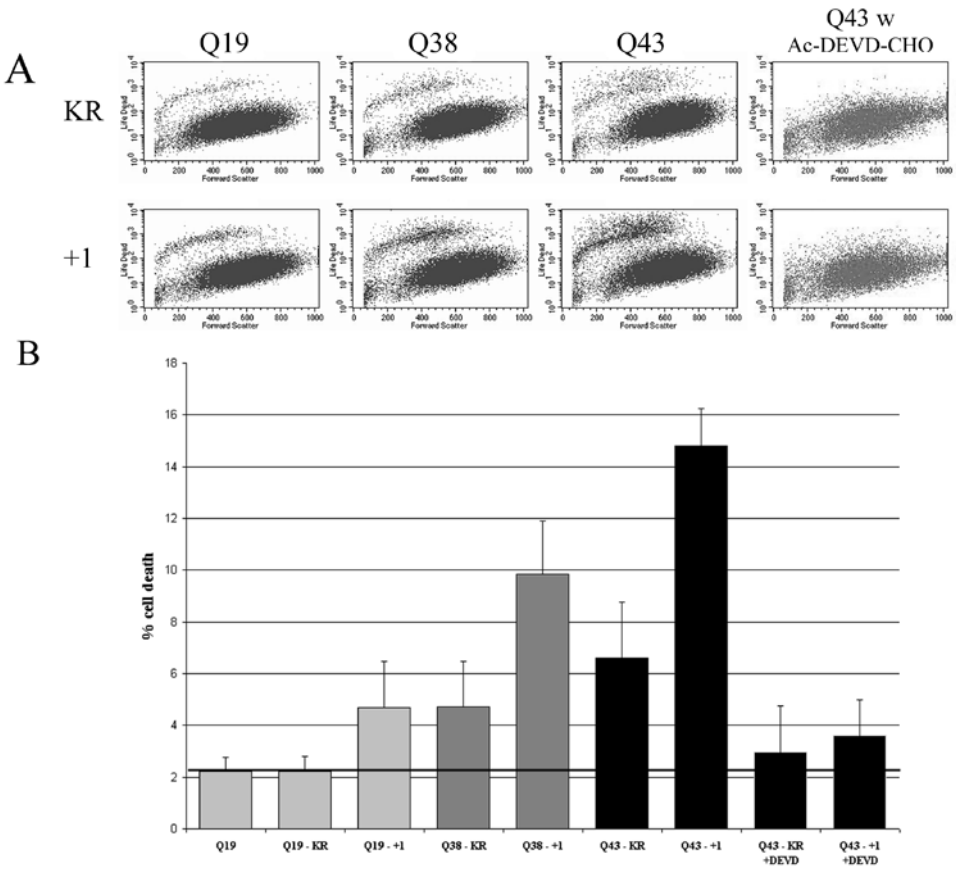


*Cell death of differentiated SH-SY5Y neuroblastoma cells, as assessed by a cell survival assay 6 days after infection, with constructs with 19, 38 or 43 glutamines (HA-Q-GFP) in combination with UBB$^{+1;K29,48R}$ (KR) as a control or UBB$^{+1}$ (+1). Polyglutamine-GFP positive cells were analyzed by flow cytometry for conversion of red-fluorescent dye (A; representative FACS analysis). Scatter plots clearly show the differential distribution of living cells (lower population) and dead cells (higher population; bright red-fluorescent). The bars (B) show the percentage of cell death that was observed under different conditions. Q19 shows the background percentage of cell death due to infection or culturing and no increase was observed in combination with UBB$^{+1;K29,48R}$ (B). The horizontal line signifies the percentage of background cell death. A minor increase in cell death was observed with expansion of the polyglutamine repeat. Co-infection with UBB$^{+1}$ caused a small increase in cell death of Q19, but a marked increase was observed with constructs of both 38 and 43 glutamines. Statistical analysis by two-way ANOVA showed a strong synergistic effect of UBB$^{+1}$ on cell death by expanded polyglutamines (P<0.001). Caspase inhibition with Ac-DEVD-CHO resulted in a marked decrease of cell-death due to UBB$^{+1}$ as well as due to expanded polyglutamines. Statistical analysis revealed no significant increase in cell-death in comparison to the background level. All experiments were performed in triplicate.*

To investigate the effect of the expression of the different proteins on the viability of neuroblastoma cells we performed a cell-survival assay (Figure 5). The scatter plots show a representative FACS analysis of the polyglutamine expressing cells (Figure 5A). Dead cells show a marked increase in red-fluorescence due to conversion of the reactive dye (higher population). Cell death due to Q19 represents the background level of cell death due to infection and culturing of the cells, whereas Q19 itself is not toxic (de Cristofaro et al., 1999). Combination of Q19 with $UBB^{+1;K29,48R}$, which was used as a control, does not affect cell death. Expansion of the polyglutamine repeat resulted in a moderate increase in cell death when combined with $UBB^{+1;K29,48R}$. We measured a small but significant increase for the plasmid with 38 glutamines, whereas the expansion to 43 caused a significant three-fold increase in cell death. Upon addition of $UBB^{+1}$ a moderate and significant increase in cell death was found for the Q19 construct. In contrast to previous experiments (De Vrij et al., 2001), lentiviral transduction resulted in only moderate cell death for $UBB^{+1}$ (Figure 4B) due to degradable levels of $UBB^{+1}$ protein (Fischer et al., 2003). However, $UBB^{+1}$ in combination with longer glutamine repeats caused a much more pronounced increase in cell death for Q38 as well as for Q43 constructs. Statistical analysis by two-way ANOVA confirmed that the combination of $UBB^{+1}$ with constructs of 38 and 43 glutamines has a pronounced, highly significant synergistic effect on the cell death mechanism ($P<0.001$). This synergistic effect manifests itself as an increase of the absolute effect of $UBB^{+1}$ on cell death with increasing length of the Hungtingtin fragment. Caspase inhibition by Ac-DEVD-CHO resulted in a marked decrease in cell-death in our polyglutamine model, indicating that cell death due to $UBB^{+1}$ as well as due to expanded polyglutamines occurs via an apoptotic pathway (Figure 4B). The percentage of cell death with caspase inhibitor did not significantly increase above the background level.

## Discussion

Previously we reported that the accumulation of $UBB^{+1}$ in tauopathies is a marker for proteasomal dysfunction (Fischer et al., 2003). Here we show that this accumulation is not only indicative of proteasome impairment, but that $UBB^{+1}$ apparently also contributes to the pathogenesis of polyglutamine diseases. The accumulation of $UBB^{+1}$ protein enhances aggregate formation in a cellular model of polyglutamine disease. In addition, the toxicity of $UBB^{+1}$ in combination with expanded polyglutamines is not only additive but clearly works synergistically. It thus suggests that both toxic proteins somehow intervene with the same or analogous pathways to compromise cellular function, and eventually cause cell death.

Molecular misreading of the *UBB* gene is a general process that occurs both in neurological diseases and in control individuals (Fischer et al., 2003). We performed a ligase chain reaction (LCR), as described earlier, to confirm the presence of $UBB^{\Delta GU}$ transcripts in the mRNA from frontal cortex tissue of three different HD patients

(data not shown) (Fischer et al., 2003). The GU deletion was present in all HD patients tested, indicating that at the level of the mRNA there is no difference between HD patients, controls or any of the previously tested neurological diseases (Fischer et al., 2003). Differences in $UBB^{+1}$ staining are probably the result of decreased proteasomal activity due to disease-related proteins or ageing (Carrard et al., 2002; Fischer et al., 2003; Keck et al., 2003; Keller et al., 2000; Zhou et al., 2003). Neurological diseases such as Parkinson disease, in which impairment of the proteasome is not demonstrated, do not lead to $UBB^{+1}$ accumulation (Fischer et al., 2003; Furukawa et al., 2002).

Both HD and SCA3 form NIIs, and we demonstrated here that, independent of their protein context, huntingtin and ataxin-3 respectively, these aggregates contain $UBB^{+1}$ (Figure 1). Moreover, $UBB^{+1}$ not only localizes to the inclusions; the cytoplasmic immunoreactivity for this aberrant protein is increased as well (Figure 1A), indicating high protein levels that potentially impair the proteasome. Accumulation of $UBB^{+1}$ reflects in vivo proteasomal impairment in the polyglutamine disorders, which is in agreement with previous in vitro results (Bence et al., 2001; Chai et al., 1999; Verhoef et al., 2002). What is striking is the accumulation of $UBB^{+1}$ in all tested HD and SCA3 patients, irrespective of polyglutamine length and age, showing that $UBB^{+1}$ can already accumulate at a young age (Figure 1B). The high stability of ubiquitinated $UBB^{+1}$ contributes to the accumulation in disease, and it has been suggested that even low levels of misreading can result in toxic protein levels (Lam et al., 2000). We did not find $UBB^{+1}$ in SCA6, suggesting proper functioning of the proteasome in this channelopathy. Indeed the proteasome has not been implicated in disease progression in SCA6, and the inclusions, which are only present in the cytoplasm, are not ubiquitinated (Ishikawa et al., 1999).

Although the mechanism by which different cellular proteins are recruited into NIIs is unknown, the presence of $UBB^{+1}$ in NIIs in human tissue and in a cellular model implicates a similar mechanism. Accumulation of $UBB^{+1}$ will probably start in the cytoplasm, followed by translocation into the NIIs. Interestingly, we showed that ubiquitination on lysine 29 or 48 is not only required for degradation of $UBB^{+1}$, in agreement with previous results (Lindsten et al., 2002), but is also needed for its translocation to the inclusions. Polyubiquitin chains of targeted proteins are bound to the S6a regulatory subunit of the 19S cap, and it is likely that both the $UBB^{+1}$ resistance to degradation and its proteasomal impairment resemble binding to this subunit but lack of processing through the 20S core (Lam et al., 2002; Lam et al., 2000). Components of the proteasome, and especially the 19S cap structure, have been shown to be present in NIIs and could thus explain the localization of $UBB^{+1}$ into inclusions (Chai et al., 1999; Schmidt et al., 2002).

In addition to human brain material, we also found accumulation and co-aggregation of the proteasome substrate $UBB^{+1}$ with expanded polyglutamines in a cellular model (Figure 2). Moreover, the proteasome inhibitor $UBB^{+1}$ causes an increase in aggregate formation of expanded polyglutamines (Figure 3 and 4). We suggest that inhibition of

the degradation machinery is central to development of polyglutamine diseases and causes accumulation of different aberrant proteins.

We demonstrated that, UBB$^{+1}$ not only increases aggregate formation, but also has a synergistic effect on apoptotic cell-death by expanded polyglutamines (Figure 5). Ubiquitinated UBB$^{+1}$ and expanded polyglutamine proteins have been shown to inhibit the proteasome in vitro (Bence et al., 2001; Lindsten et al., 2002; Verhoef et al., 2002), and we demonstrated here that both factors enhance the effect of the other aberrant protein. The mutual decrease of proteasome activity probably leads to further accumulation of aberrant proteins, and eventually cell death. The fact that ubiquitination of UBB$^{+1}$ is required for its proteasomal inhibition (Lindsten et al., 2002), its toxicity (De Vrij et al., 2001) and its contribution to aggregate formation and polyglutamine-induced cell death suggests that polyubiquitination is a prerequisite for both aggregate formation and cell-death.

Although the genetic basis of polyglutamine diseases is known, a number of questions remain unanswered as to the precise cause of toxicity and whether aggregates are either beneficial or toxic (Michalik and Van Broeckhoven, 2003). Even between individuals with similar repeat length, there are differences as to the age at onset, the progression, and the extent of atrophy (Halliday et al., 1998; McNeil et al., 1997; Rubinsztein et al., 1996; Zoghbi and Orr, 2000). Recent reports indicate that genetic and familial factors account for a great deal of variation of the age at onset in HD (Li et al., 2003; Wexler et al., 2004). Possible candidates include proteasome subunits and cellular chaperones (Chan et al., 2002; Willingham et al., 2003) and, as described in the present paper, also factors such as UBB$^{+1}$ can act as modifiers of both the onset and severity of the disease.

From the present study it is evident that UBB$^{+1}$ not only accumulates in polyglutamine diseases, indicating impairment of the proteasome, but probably plays a role in neurodegeneration itself. In addition to co-aggregation with polyglutamine proteins, ubiquitinated UBB$^{+1}$ synergistically aggravates polyglutamine-induced aggregate formation, and especially cell-death. Targeting of UBB$^{+1}$ to the proteasome by ubiquitination is thereby required for degradation, toxicity and colocalization with the NIIs. Consequently, the accumulation of UBB$^{+1}$ in HD and SCA3 post-mortem tissue, in both the inclusions and the cytoplasm of neurons, implicate UBB$^{+1}$ as an aggravating factor in polyglutamine-induced neurodegeneration, and clearly identifies an important role for the ubiquitin-proteasome system in polyglutamine diseases. These results indicate that proteasomal activation or removal of its blockades is a promising avenue for the treatment of polyglutamine diseases.

***Table 1. Clinicopathological information of Huntington, SCA 3 and SCA 6 patients.***

| Patient number | Age | Sex | Postmortem delay (h) | Brain weight (g) | Fixation duration (days) | CAG repeat expansion | Vonsattel grade | Areas investigated |
|---|---|---|---|---|---|---|---|---|
| **HD*** | | | | | | | | |
| 1 | 11 | f | 21 | 1240 | 21 | 22 - 84 | 3 | frontal cortex |
| 2 | 20 | f | 36 | 860 | 21 | 17 - 86 | 4 | frontal cortex |
| 3 | 33 | f | 144 | 1220 | 122 | 20 - 52 | 3 | frontal cortex |
| 4 | 39 | m | 10 | na | 363 | 15 - 59 | 4 | frontal cortex, striatum |
| 5 | 40 | m | 16 | 1400 | 124 | 10 - 41 | 3 | frontal cortex |
| 6 | 41 | f | 24 | 1150 | 42 | 16 - 46 | 3 | frontal cortex, striatum |
| 7 | 49 | m | 120 | 1120 | 186 | 21 - 51 | 4 | frontal cortex |
| 8 | 49 | f | na | na | 186 | 17 - 47 | 3 | frontal cortex |
| 9 | 50 | m | 4 | 1230 | 31 | 20 - 47 | 3 | frontal cortex |
| 10 | 51 | m | 4 | 1260 | 2 | 27 - 45 | 3 | frontal cortex |
| 11 | 51 | f | 5 | 900 | 14 | 19 - 46 | 4 | frontal cortex |
| 12 | 51 | f | 74 | 1100 | na | 15 - 43 | 3 | frontal cortex |
| 13 | 52 | f | 20 | 840 | 31 | 16 - 53 | 4 | frontal cortex |
| 14 | 55 | m | 24 | 1250 | 124 | 22 - 47 | 2-3 | frontal cortex |
| 15 | 56 | m | 32 | 1250 | 2 | 18 - 49 | 3 | frontal cortex |
| 16 | 57 | f | 72 | 1200 | 162 | 16 - 43 | 3 | frontal cortex |
| 17 | 58 | f | 34 | 1170 | 7 | 24 - 43 | 3 | frontal cortex |
| 18 | 60 | m | 12 | 1200 | 248 | 20 - 43 | 3 | frontal cortex |
| 19 | 60 | m | na | na | 35 | 26 - 47 | 4 | frontal cortex |
| 20 | 61 | f | 17 | 1050 | na | 17 - 45 | 3 | frontal cortex |
| 21 | 61 | f | 24 | 840 | 21 | 21 - 47 | 4 | frontal cortex |
| 22 | 62 | m | 12 | 1200 | 62 | 20 - 43 | 3 | frontal cortex |
| 23 | 63 | f | 10 | 1100 | 58 | 17 - 45 | 3 | frontal cortex, striatum |
| 24 | 64 | f | 60 | 1080 | 7 | 19 - 42 | 3 | frontal cortex |
| 25 | 66 | m | 28 | 1125 | 78 | 21 - 40 | 3-4 | frontal cortex |
| 26 | 66 | f | na | 950 | 107 | 20 - 44 | 3-4 | frontal cortex, striatum |
| 27 | 68 | f | 12 | 1130 | 62 | 20 - 42 | 3 | frontal cortex |
| 28 | 69 | f | 24 | na | 155 | 21 - 40 | 3 | frontal cortex |
| 29 | 69 | m | 48 | 1200 | 62 | 16 - 42 | 3 | frontal cortex |
| 30 | 76 | m | 14 | 970 | 81 | 15 - 46 | 3 | frontal cortex |
| **SCA3*** | | | | | | | | |
| 31 | 34 | m | na | 1598 | 28 | 20 - 75 | | medulla oblongata |
| 32 | 51 | m | 24 | 1244 | 21 | 27 - 72 | | hippocampus, mesencephalon |
| 33 | 59 | f | 12 | 1290 | 21 | 20 - 72 | | hippocampus, pons |
| 34 | 62 | m | 21 | 1236 | 21 | 23 - 70 | | hippocampus, pons |
| 35 *** | 65 | m | <12 | 1258 | 28 | 27 - 72 | | pons |
| 36 *** | 66 | m | 14 | 1220 | 21 | 24 - 70 | | pons |
| **SCA6*** | | | | | | | | |
| 37 | 69 | m | 46 | 1395 | 28 | ** | | hippocampus, cerebellum |
| 38 | 76 | m | 24 | 1418 | 120 | 22 | | cerebellum |

* all cases positive with htt-07, ataxin-3 and A6RPT-C respectively
** not available, but most probably 21 or 22
*** brothers
na - not available

## Materials and Methods

### *Patients*

Autopsy material was obtained from the Huntington bank (Leiden University Medical Center, The Netherlands) for HD cases, and the Laboratory of Pathology East Netherlands (Enschede, The Netherlands) and University Hospital Groningen (Groningen, The Netherlands) for SCA cases (for details see Table 1). We analyzed striatal tissue from 4 different HD patients and frontal cortex tissue of in total 30 HD patients with polyglutamine expansion of various lengths. Furthermore, we examined the hippocampus, pons, mesencephalon and medulla oblongata of 6 different SCA3 patients and the hippocampus and cerebellum of two SCA6 patients. All brain areas were fixed in formaldehyde and subsequently embedded in paraffin.

### *Immunohistochemistry*

Paraffin sections (6 μm) were immunohistochemically labeled with different antibodies using the peroxidase-anti-peroxidase method with nickel intensification as described previously (van Leeuwen et al., 1998). The 1C2 monoclonal antibody against expanded polyglutamine repeats (Trottier et al., 1995) (1:10,000; Chemicon, Temecula, USA), polyclonal Htt-07 antiserum against the N-terminus of huntingtin (1:100)(Maat-Schieman et al., 1999), polyclonal anti-ataxin-3 antibody (1:2000) (Paulson et al., 1997) and polyclonal A6RPT-C against the C-terminus of the α1A-subunit of the voltage dependent Ca channel (1:100) (Ishikawa et al., 1999) were used for the detection of the respective disease proteins. $UBB^{+1}$ was detected using antisera against the C-terminal part of the protein (Ubi2A, 1:1000, bleeding 020698 and Ubi2+1, 1:1000, bleeding 010994; see references for details on epitope and specificity (Fischer et al., 2003; van Leeuwen et al., 1998)).

For double stainings, we subjected paraffin sections to irradiation with a broad spectrum lamp for at least 24 hours to reduce autofluorescence (Hol et al., 2003; Neumann and Gabel, 2002). We then deparaffinized sections and incubated them with the first antibodies overnight in a humid chamber at 4°C. We enhanced the $UBB^{+1}$ signal using the avidin-biotin-complex and tyramine procedure (Kerstens et al., 1995) (Sigma-Aldrich, St.Louis, USA) and stained with streptavidin-conjugated-Cy5 (Jackson Laboratories, West Grove, USA). 1C2 was directly visualized using donkey-anti-mouse-Cy2. Signal specificity was demonstrated by swapping fluorescent dyes and omission of primary antibodies to exclude aspecific staining or signal enhancement. Images were obtained using a confocal laser scanning microscope (Zeiss 510).

### *Cell lines:*

HeLa cells were cultured in low-glucose Dulbecco's modified Eagle medium containing 10% fetal calf serum, supplemented with 10000 IU/ml penicillin and 10

mg/ml streptomycin (all Invitrogen, Grand Island, NY). Cells were cultured on 0.2% gelatin-coated glass coverslips in 24-well plates (Nunc, Roskilde, Denmark) 1 day before transfection.

SH-SY5Y neuroblastoma cells (ATCC:CRL-2260) were cultured in high-glucose Dulbecco's modified Eagle medium containing 15% fetal calf serum, supplemented with 100 U/ml penicillin and 100 µg/ml streptomycin (all Invitrogen). Cells were cultured in 6-well plates (Nunc) 1 day before infection. Caspase inhibition was performed by addition of 100 µM Ac-DEVD-CHO (Sigma) to the culture medium every two days.

### *Transfections*

We performed transfections with the calcium-chloride method, using 0.5µg plasmid DNA of each of the respective plasmids for 24 well plates (Naldini et al., 1996). Polyglutamine plasmids containing a truncated *huntingtin* fragment with different polyglutamine repeats (19, 38 and 43) flanked by a HA tag and green fluorescent protein (GFP) reporter sequence were provided by Dr. de Christofaro (de Cristofaro et al., 1999). Vectors for ubiquitin, $UBB^{+1}$ and a lysine mutant of $UBB^{+1}$ in which both lysine 29 and 48 are mutated into an arginine residue ($UBB^{+1;K29,48R}$) were described earlier (Lindsten et al., 2002).

Cells were fixed 4 days after transfection and stained for $UBB^{+1}$ (Ubi3, 1:500, bleeding 050897 (De Vrij et al., 2001)). Subsequently cells were incubated with donkey-anti-rabbit-Cy3 (1:200; Jackson laboratories) and ToPro-3 nuclear staining (1:200, Molecular Probes, Leiden, The Netherlands). After staining for $UBB^{+1}$, pictures were obtained using a confocal laser scanning microscope (Zeiss 510).

### *Infections*

cDNAs for $UBB^{+1}$, $UBB^{+1;K29,48R}$, HA-Q19-GFP, HA-Q38-GFP and HA-Q43-GFP were cloned in the lentiviral transfer plasmid pRRLsin-PPThCMV-GFP-pre (Naldini et al., 1996). VSV-G pseudotyped lentivirus was produced by cotransfection of the transfer plasmid and helper plasmids (pCMVdeltaR8.74 and pMD.G.2) in 293T cells. Medium was harvested 24 and 48 h after transfection and concentrated by ultracentrifugation. Virus pellets were resuspended in PBS containing 0.5% bovine serum albumin (Sigma). Stocks were titered with a HIV-1 p24 coat protein ELISA (NEN Research, Boston, USA). Lentiviral vectors were used to infect SH-SY5Y neuroblastoma cells at a multiplicity of infection of 50.

### *Quantification of cells*

For aggregate formation, cells were counted manually at different time intervals after infection. The number of aggregate forming cells was quantified in three randomly

selected fields per experiment. Experiments were performed in triplicate and statistics was performed using three-way ANOVA, testing the interaction between repeat expansion, UBB$^{+1}$ protein expression and time course. UBB$^{+1}$ immunopositive cells, were counted after fixation and immunofluorescent staining for UBB$^{+1}$. The number of UBB$^{+1}$ immunopositive cells were quantified in three randomly selected fields per experiment. Experiments were performed in triplicate and statistics was done using one-way ANOVA, testing the significance of repeat expansion on UBB$^{+1}$ accumulation.

### *Western blots*

We harvested neuroblastoma cells (SH-SY5Y) 6 days after infection in cold PBS. Cell-pellets were resuspended in lysis-buffer (1% NP40, 0.1 M NaCl, 0.01 M Tris-HCl pH 8.0, 1 mM EDTA pH 8.0) containing protease inhibitors; 100 mM PMSF and 10 mg/ml leupeptin. We performed cell-lysis at 4°C for 30 minutes and passed samples through a 25G needle to ensure complete lysis. All samples were loaded onto SDS-PAGE gels and transferred semi-dry onto nitrocellulose (Schleicher & Schuell, Dassel, Germany). Polyglutamine proteins were detected using a monoclonal antibody directed against the HA tag (12CA5, 1:100, culture supernatant) (Field et al., 1988). Blots were additionally probed with a monoclonal β-actin antibody (JLA2.0, 1:500; Developmental Studies Hybridoma Bank, Iowa, USA) as a control for the amount of cell-lysate loaded. Subsequently, blots were incubated with anti-mouse HRP (1:1000; DAKO, Glostrup, Denmark) followed by Lumilight ECL (Perkin Elmer, Norwalk, USA) chemiluminescence. The integrated optical density of the bands was determined by image analysis with Image Pro Plus.

### *Cell survival assay*

We assessed SH-SY5Y cell-survival using a Life-Dead® kit (red fluorescence; Molecular Probes, Leiden, The Netherlands) and analyzed on a flow cytometer (Becton Dickinson, Palo Alto, USA) according to the manufacturers protocol. In short, we harvested lentivirally infected cells (see before) 6 days after infection, washed in PBS and incubated them for 30 minutes with the fluorescent reactive dye. Subsequently, we fixed cells with 4% formaldehyde for 15 minutes and resuspended in PBS-BSA (1x PBS pH-7.6, 0.5% BSA, 0.1% $NaN_3$). We analyzed polyglutamine-GFP expressing cells by flow cytometry for conversion of the Life-Dead® kit reactive dye. At least $10^4$ polyglutamine-GFP positive cells were examined per sample. Dead cells showed a marked increase of red-fluorescence over living cells due to conversion of the dye (Figure 4A). Experiments were performed in triplicate and statistics were done using two-way ANOVA, testing the interaction between UBB$^{+1}$ protein expression and repeat expansion.

## Acknowledgements

We thank Drs. T. de Christofaro (Universita di Napoli "Federico II", Naples, Italy) for sending of polyglutamine plasmids, L. Naldini (Institute for Cancer Research, University of Torino Medical School, Italy) for lentiviral plasmids, H. L. Paulson (University of Iowa, Iowa, USA) for the ataxin-3 antibody, K. Ishikawa (Medical and Dental University, Bunkyo-ku, Japan) for A6RPT-C staining, M. Losekoot (Molecular Genetics Laboratory, Leiden, The Netherlands) for CAG determinations, N. Dantuma (Karolinska Institutet, Stockholm, Sweden) and Department of Experimental Internal Medicine (Amsterdam Medical Center, Amsterdam, The Netherlands) for technical advice and use of FACS equipment, J. A. Sluijs (Netherlands Institute for Brain Research, Amsterdam, The Netherlands) for virus production, J. J. van Heerikhuize and R. F. Roelofs (Netherlands Institute for Brain Research, Amsterdam, The Netherlands) for technical advice, W. Verweij (Netherlands Institute for Brain Research, Amsterdam, The Netherlands) and J. M. Ruijter (University of Amsterdam, Amsterdam, The Netherlands) for critical remarks and statistical advice.

Financial support was given by the Prinses Beatrix Foundation (MAR 99-0113), the 5th Framework "Quality of life and management of living resources" EU grant (QLRT-1999-02238), Hersenstichting Nederland (Grant H00.06) and Platform Alternatieven voor Dierproeven (#98-19).